JOURNAL OF GENERAL VIROLOGY

RESEARCH ARTICLE

Dall'Ara *et al.*, *Journal of General Virology* 2024;105:001950

DOI 10.1099/jgv.0.001950

MICROBIOLOGY SOCIETY

Analysis of the relative frequencies of the multipartite BNYVV genomic RNAs in different plants and tissues

M. Dall'Ara[1,*,†], Y. Guo[1,†], D. Poli[1], D. Gilmer[2,*] and C. Ratti[1,*]

Abstract

Multipartite virus genomes are composed of two or more segments, each packaged into an independent viral particle. A potential advantage of multipartitism is the regulation of gene expression through changes in the segment copy number. Soil-borne beet necrotic yellow vein virus (BNYVV) is a typical example of multipartism, given its high number of genomic positive-sense RNAs (up to five). Here we analyse the relative frequencies of the four genomic RNAs of BNYVV type B during infection of different host plants (*Chenopodium quinoa*, *Beta macrocarp*a and *Spinacia oleracea*) and organs (leaves and roots). By successfully validating a two-step reverse-transcriptase digital droplet PCR protocol, we show that RNA1 and -2 genomic segments always replicate at low and comparable relative frequencies. In contrast, RNA3 and -4 accumulate with variable relative frequencies, resulting in distinct RNA1 : RNA2 : RNA3 : RNA4 ratios, depending on the infected host species and organ.

INTRODUCTION

Segmentation of hereditary material into multiple entities appears to be a common feature for cellular organisms [1–3] that is also found in some viruses. Viral genome segmentation is found in ~13% of all viral genera, infecting heterogeneous hosts such as bacteria, animals, plants and fungi [4]. Excluding rare examples [5], animal and bacterial viruses with a split genome co-package their complete set of genomic segments into a single virion or enveloped entity; these are described as segmented viruses. Split genomes are also found for fungi and plant viruses that can adopt a multipartite strategy; their genomic segments are separate from one another within independent particles [4]. Thirteen out of 24 plant viral families possess species with multipartite genome organization, making multipartitism a notable characteristic of plant viruses [4]. This has raised questions about the possible benefits and costs of multipartism and why this strategy is so prevalent among plant viruses. Opting for smaller genomic segments instead of a single large genomic nucleic acid can confer a significant advantage. Incomplete molecules exhibit higher replication fidelity compared to their complete counterparts. Specifically, a molecule encoding just one functional gene presents a smaller target for deleterious mutations, in contrast to a molecule encoding multiple functional genes. This underscores the importance of complementation in multicomponent viruses, as it becomes both a necessity and an evolutionary advantage. In cases where a genomic segment undergoes deleterious mutation, it can be replaced by a functional one, thus ensuring the virus's viability [6–8]. Indeed, competition experiments between monopartite and spontaneous bipartite forms of foot-and-mouth disease virus [9] evidenced fitness advantages for the segmented variant, at least in cell culture. This fitness was linked to the higher particle thermal stability rather than a faster kinetics of RNA synthesis. Furthermore, a sufficiently high multiplicity of infection (m.o.i.) was considered to be a requirement for persistence [10]. Split genomes in complementary modules could also confer a reassortment capacity to co-infecting similar viruses, leading to the selection of reassortant progeny with potential fitness advantages [11].

Received 05 May 2023; Accepted 19 December 2023; Published 10 January 2024

Author affiliations: [1]DISTAL-Plant pathology, University of Bologna, Viale G. Fanin, 40, 40127 Bologna, Italy; [2]Institut de biologie moléculaire des plantes, CNRS, Université de Strasbourg, France.

***Correspondence:** M. Dall'Ara, mattia.dallara5@unibo.it; D. Gilmer, david.gilmer@ibmp-cnrs.unistra.fr; C. Ratti, claudio.ratti@unibo.it

Keywords: multipartitism; RNA virus; RT-ddPCR; set point genome formula.

Abbreviations: CP, coat protein; LLQ, low limit of quantification; m.o.i., multiplicity of infection; PE, percent error; RSD, relative standard deviation; RT-ddPCR, reverse transcriptase droplet digital PCR; SECCC, sieve element companion cell complex; SGF, set point genomic formula; TGB, triple gene block.

†These authors contributed equally to this work

One supplementary figure and four supplementary tables are available with the online version of this article.

If the above-mentioned benefits are still debated [12] and also referred to segmented viruses, recent studies on multipartite and segmented viruses have shown that, during host infection, the relative frequencies of encapsidated genomic fragments converge to a set point genomic formula (SGF) [13–19]. The distinct segments accumulate differently, with some more abundant than others depending on the infected host. This suggests that partition could have evolved to regulate gene expression in different contexts. However no direct demonstration of such adaptation has been provided so far. Viruses selected for these studies were the nanoviridae *Faba bean necrotic stunt virus* (FBNSV) and *Banana bunchy top virus* (BBTV) [14, 15, 17], the bromoviridae *Alfalfa mosaic virus* (AMV) and *Cucumber mosaic virus* (CMV) [16, 19], the phenuiviridae *Rice stripe virus* (RSV) [18] and the bidnaviridae *Bombyx mori bidensovirus* (BmBDV) [13]. Each of them represents a distinct multipartite viral example with peculiar host and genomic characteristics. BmBDV is one of the few animal multipartite viruses described so far [12, 13], while FBNSV, BBTV, AMV, CMV and RSV belong to the most representative multipartite virus group comprising plant viruses. With eight circular single-stranded DNAs, FBNSV has the largest number of genomic segments among multipartite plant viruses, but such a genome type is only common within 17% of multipartite families [4]. RSV, an RNA virus with four negative-sense single-stranded genomic segments, is a typology represented solely by the genus *Tenuivirus* and two genera of the family *Rhabdoviridae* [4]. By contrast, AMV and CMV possess a tripartite positive-sense single-stranded RNA genome ssRNA(+); an organization conserved within 74% of plant multipartite genera [4]. *Bromoviridae* genome organization is characterized by the distribution of essential genes (for replication, gene-silencing suppression and movement) among all three segments and has no equivalent with other multipartite plant viruses, except for *Hordeivirus* and *Pomovirus* (*Virgaviridae*) [4]. In fact, multipartite plant viruses with a ssRNA(+) genome mainly present the segregation of essential genes in two segments and, when present, extra segments carry so-called 'unessential' genes linked to host or vector related functions usually needed to optimize infection [4]. The *Beet necrotic yellow vein virus* (BNYVV), which belongs to the family *Benyviridae*, could be considered to be a representative member of this group of viruses as it has the highest number of genomic RNAs organized in two essential segments, common to other benyvirus species, and up to three accessory RNAs [20]. European isolates typically possess four genome RNAs, while the presence of a fifth RNA (RNA5) is described in French and Asian isolates [21]. RNA1 encodes the viral replicase, while RNA2 directs the synthesis of the major (CP) and minor (p75) capsid proteins of the rod-shaped particles [20]. Thanks to the synthesis of subgenomic RNAs, the proteins required for the cell-to-cell movement (triple gene block, TGB) and the suppression of the host post-transcriptional gene silencing (p14) are produced [20]. The RNA3 species is involved in long-distance movement and encodes the pathogenic determinant of the rhizomania disease on sugar beet (p25) while RNA4 is involved in the efficiency of virus transmission by the soil-borne vector *Polymyxa betae* [20]. In genotypes in which it is present [21], the RNA5 is responsible for symptoms worsening [18]. The natural host range of BNYVV is very narrow and limited to species from the genera *Beta* or *Spinacea*. Species of *Chenopodium* are infected in laboratory conditions, mostly only locally and mechanically (e.g. *C. quinoa*) [20].

The aim of this study was to determine whether BNYVV gene copy number changes in a host- and organ (leaf or root)-dependent manner. We determined the segment relative accumulations of the European type B of BNYVV, of which we possess the infectious cDNA clones, in leaves and roots of *Spinacia oleracea* and *Beta macrocarpa* and within *C. quinoa* local lesions using a validated protocol of two-step reverse transcriptase droplet digital (RT-dd)-PCR. The results obtained are discussed with regard to other known multipartite viruses.

METHODS

Host species and virus inoculation

B. macrocarpa, *S. oleracea* cv. Viking and *C. quinoa* were chosen as experimental hosts. Plants were grown with a 16/8 h day/night photoperiod, a temperature of 22/18°C day/night and 70% hygrometry. A common source of inoculum was provided by *B. macrocarpa* plants previously agro-infected with four *Agrobacterium tumefaciens* cell cultures, each containing one of the four plasmids, allowing *in vivo* expression of infectious B type BNYVV RNA as described previously [22]. *B. macrocarpa*-infected systemic tissues were used to perform foliar rub inoculation in 10 mM phosphate buffer, pH 7.0, in new and healthy *B. macrocarpa, S. oleracea* and *C. quinoa* plants. *C. quinoa* leaves were also infected with a second source of inoculum. This inoculum consisted of 100 µl of *B. macrocarpa*-infected sap enriched with 2 µg of RNA2 produced *in vitro* by run-off transcription of the full-length linearized T7 cDNA clone pB214 [23].

BNYVV standard production and two-step RT- ddPCR reaction

Standard BNYVV RNAs were obtained by transcription of the full-length cDNA clones pB214 (RNA2), pB35 (RNA3) and pB45 (RNA4) [23, 24]. Since pB15 (RNA1) [23] run-off transcription produced a significant amount of incomplete RNA due to premature T7 polymerase stops, the last 2991 nucleotides were amplified using 3755F- and 6746R-specific RNA1 primers (Table 1) with GoTaq Long PCR Master Mix (Promega) and cloned in pGEM-T Easy Vector (Promega), verifying the correct insert orientation through Sanger sequencing. The resulting *Hin*dIII-linearized plasmid was transcribed *in vitro* as described

Table 1. Primers and probes used to amplify and detect BNYVV RNAs in RT-ddPCR experiments. Primers used to clone the 3' portion of BNYVV RNA1 in pGEM-T Easy Vector (3755F and 6746R) are included

RNA	Primers	TaqMan probes
1	**3755F** CGGAAGAACTCGAAAGAAGG	
	6746R AAGCTTTTTTTTTTTTTTTTATATCAATATACTG	
1	**3946F** TGGTTTCACAAGGAGATGTCGTT	**3944 FAM**-TTTTGGACATAGCACGTGTGGAAAACGATA
	4024R TCTGCACAATCAAAGGCATCA	
2	**662F** TGGACCCGGGATAAATTTGA	**653 HEX**-ACCGGTTCAAATTACCATGGACACCTGTT
	734R CGGGTGGACTGGTTCTACCTT	
3	**54F** ATATGTGAGGACGCTAGCCTGTT	**84 FAM**- CTGACCGACCAAATCCAAGCGAGCTTAAT
	172R TGAAACGATGGAGTCACTATGCTT	
4	**415F** TCCTCCTTTGATACGTCATGAAGA	**445 HEX**-TGATTGTACTGCTAGGATGGTGCA
	490R CAATGGGCCAATCTCAATCC	

by Quillet *et al* [23] to produce a 3067 nt long RNA. After DNA removal with RQ1 RNase-Free DNase (Promega), RNAs were purified by phenol/chloroform extraction and NH_4OAc/EtOH precipitation prior to analysis by agarose gel electrophoresis and quantification by Qubit 3.0 fluorometer with an RNA Broad-Range Assay kit (Life Technologies). All enzymatic reactions were carried out according to the manufacturer's protocol. The molecular concentration of each transcript was determined using an online calculator tool (http://endmemo.com/bio/dnacopynum.php) and a standard dilution of 20×10^3 molecules μl^{-1} for each RNA species was produced after analysing and redefining the exact copy numbers by one-step RT-ddPCR. Copy number underestimations compared to Qubit quantification have been associated with the RNA degradation rate of the 'non-certified' standard used. Serial dilutions were then applied to obtain 20×10^2, 20×10 and 20 molecules μl^{-1} for each RNA. Combinations of all transcripts were mixed or not with 100 pg of total RNAs extracted from leaf or roots of healthy *S. oleracea*, *B. macrocarpa* and *C. quinoa* plants. To quantify standards and BNYVV genomic RNAs, primer and TaqMan probes (labelled with FAM and HEX fluorophores, Table 1 were designed to avoid the targeting of subgenomic RNA2 and noncoding RNA3 species. Primer specificity was successfully verified by performing two-step RT-ddPCR assays using a mix of standard dilutions with or without the specific BNYVV RNA targets as templates. One- and two-step RT-ddPCRs for all the BNYVV RNAs were performed in independent reactions. For one-step RT-ddPCR reaction 1 µl standard solution template was added to 19 µl of the following RT-ddPCR mixture: 5 µl 4× One-Step RT-ddPCR Advanced kit for probes (Bio-Rad); 2 µl reverse transcriptase 20 U μl^{-1} (Bio-Rad); 1 µl DTT 300 mM; 0.5 µl BNYVV forward primer (20 µM); 0.5 µl BNYVV reverse primer (20 µM); 1 µl BNYVV FAM or HEX probe (4 µM); DNase/RNase free water to 19 µl. RT-PCR reactions were performed after droplet generation. After 30 min of reverse transcription, PCR thermal cycling conditions were set as follows: 10 min of polymerase activation at 95°C; 40 cycles of 95°C for 30 s (denaturation) and 59°C for 60 s (annealing/extension); 10 min of enzyme inactivation at 98°C. Ramp rate was adjusted to 2°C s^{-1}. Two-step RT-ddPCR reactions were performed by mixing 1 µl of standard solution or infected plant RNA extraction templates with 4 µl of the following reverse transcriptase mixture: 1 µl 5× Reverse Transcriptase Reaction Buffer (Tris/HCl 250 mM; pH 8.3, KCl 375 mM, $MgCl_2$ 15 mM, DTT 50 mM); 0.3 µl dNTPs (10 mM each); 0.2 µl AMV RT (10 U μl^{-1}) (Promega); 0.5 µl BNYVV reverse primer (20 µM); DNase/RNase free water to 4 µl. The reverse transcription reaction was carried out at 42°C for 1 h prior to the enzyme inactivation at 90°C for 5 min. To 5 µl of each reverse transcriptase reaction, 15 µl of the following ddPCR mixture was added: 10 µl 2× ddPCR Supermix for probes (Bio-Rad); 0.5 µl BNYVV forward primer (20 µM); 1 µl BNYVV FAM or HEX probe (4 µM); DNase/RNase free water to 15 µl. PCR reactions were carried out after droplet generation with thermal cycling conditions set as explained above.

Total and encapsidated RNA extraction, preparation of samples for two-step RT-ddPCR, genomic RNA relative frequency calculation and statistical analyses

Two discs from symptomatic leaves (Ø=1 cm) and 300 mg of root tissues were collected from *B. macrocarpa*- and *S. oleracea*-infected plants at 16 and 21 days post-inoculation (p.i.), respectively, while *C. quinoa* leaf local lesions were collected separately as independent samples 7 days p.i. Samples were homogenized in 600 µl of cold Tris magnesium buffer (Tris 100 mM, $MgCl_2$ 10 mM, pH 7.5) and placed on ice. Homogenates were divided in two portions of 300 µl for total and encapsidated RNA extraction. Total RNA was immediately purified by phenol/chloroform extraction and NaOAc/EtOH precipitation from half of the homogenate. Nuclease-protected RNAs corresponding to encapsidated viral RNA were purified following the Tris magnesium protocol [25] by extracting and precipitating the remaining homogenate after 1 h of incubation at 37°C to allow vacuolar nuclease digestion of unprotected RNAs. Pellets were resuspended in 50 µl of DNase/RNase-free water and purified

RNAs were quantified with a Qubit 3.0 fluorometer. Dilutions were adjusted to analyse ~50 pg of *B. macrocarpa* and ~10 pg of *S. oleracea* and *C. quinoa* extracted RNA. Primer-independent cDNA synthesis was tested by performing RT reactions without specific primers using as template 10 pg of total RNA extracted from *C. quinoa*-infected leaf tissues. Using ddPCR we verified, in our experimental conditions, the absence of RNA secondary structures or endogenous nucleic acid molecules that can act as primers in RT reactions affecting the BNYVV positive-strand-specific quantification.

Only samples having the complete set of genomic BNYVV RNAs were used for our analyses: 16 *C. quinoa* local lesions; 18 leaf and 19 root *B. macrocarpa* samples; and 10 leaf and 10 root *S. oleracea* samples. Each BNYVV genomic RNA copy number was converted into relative frequency by dividing its value by the sum of all quantified genomic RNAs of the sample. BNYVV GFs in the different hosts and organs were determined by dividing the mean of relative frequency for each segment in total RNA extraction by the mean of relative frequency of the less abundant RNA. SGF values were rounded to the nearest half unit.

R 4.3.1 software was used to conduct the Shapiro–Wilk test to assess normality in the analysed dataset. This test covered all groups of variables in our dataset, specifically the group of relative frequencies of each genomic BNYVV RNAs in the leaves of *C. quinoa*, *B. macrocarpa* and *S. oleracea*, as well as in the roots of *B. macrocarpa* and *S. oleracea*, considering both total RNA and encapsidated RNA extraction dataset. The results of the test indicated that several variables exhibited a non-normal distribution of values (Table S1). For this reason, non-parametric tests were used to statistically analyse our dataset. The non-parametric Friedman's test was used to evaluate the statistical differences between the relative frequencies of the genomic RNAs used to calculate the SGF of BNYVV in the total RNA extracts of leaves of *C. quinoa*, *B. macrocarpa* and *S. oleracea*, as well as the roots of *B. macrocarpa* and *S. oleracea*. The main purpose of applying Friedman's test was to assess whether there was significant variation among relative frequencies of the different genomic RNAs treated as dependent variables. Friedman's test was performed with SPSS 26, and to reject the null hypothesis a P-value <0.05 was required to indicate statistical significance (Table S2). The Wilcoxon signed-rank test was utilized with SPSS 26 to evaluate statistical differences between the relative frequencies of these RNAs through all pairwise comparisons (RNA1–RNA2; RNA1–RNA3; RNA1–RNA4; RNA2–RNA3; RNA2–RNA4; RNA3–RNA4). This analysis allowed for the determination of whether the groups exhibited homogeneity or heterogeneity. Statistical significance was considered for P-values <0.008, as Bonferroni's correction was applied, setting the significance threshold at 0.05 divided by the number of comparisons made (6) (Table S3). Wilcoxon rank-sum tests were employed using R 4.3.1 software to conduct multiple comparisons of the relative frequencies of RNA1s, RNA2s, RNA3s and RNA4s across the different study groups that consider factors such as the type of inoculum, the extraction method, the organ and the infected host. To address the issue of multiple comparisons (four), we applied Bonferroni's correction, reducing the significance threshold to P<0.0125 for the null hypothesis (Table S4).

RESULTS

Validation of two-step RT-ddPCR using quantitative standards

One of the main constraints in the use of reverse transcription reaction for an RNA quantification assay is the optimization of the synthesis of a single copy of cDNA for each target RNA molecule. Complex RNA secondary structure or insufficient level of downstream RNase H activity could compromise the equimolar RNA/cDNA conversion, leading to misestimation of the RNA template copy number [26, 27]. RNA targets and reagent mix partitioning in different droplets make such concerns negligible in one-step RT-ddPCR, where each reaction event effectively assigns one unequivocal fluorescent amplitude for each molecule target. However, since RNA reverse transcription must precede cDNA droplet partitioning to prevent the conversion and the amplification of BNYVV viral complementary RNAs issued from replication intermediates, optimization and validation of the first step of a two-step RT- ddPCR is mandatory.

The quantitative linearity of two-step RT-ddPCR reactions was tested using BNYVV standard RNAs (covering four orders of magnitude from 20 to 20×10^3 molecules for each BNYVV *in vitro* transcript) containing putative RT-PCR inhibitors associated with RNA extraction from healthy leaves or roots of *B. macrocarpa*, *C. quinoa* and *S. oleracea* (mixed samples) or not. We compared the resulting copy numbers from these assays to expected copy numbers. Two replicates of RT-ddPCR tests were run for each of the 12-template matrices. As shown in Fig. 1, all of the assays demonstrated a very high degree of linearity: best fit linear lines had squared regression coefficients (R^2) greater than 0.99. The precision of the assays was evaluated by determining the relative standard deviations (RSDs) in the six replicates for each standard dilution (RSD was calculated by multiplying the standard deviation by 100 and dividing by the average). The RSDs were <20%, except for 20 BNYVV RNA standard molecules for which the RSDs were >25% (Table 2). These results attested that no remarkable inhibitory effect of environmental matrices occurred on the RNA quantifications when standard samples were mixed with total RNA extraction issued from healthy leaves or roots from *B. macrocarpa*, *S. oleracea* and *C. quinoa*. The accuracy of the assays was evaluated as the net of the percentage error (PE) between expected and observed means (|observed mean – expected value|/expected value×100). The PE was ≤11% for all the assays performed with standards that covered the range from 20×10^3 to 20×10 expected BNYVV RNA copy number (Table 2). The PE of two-step RT-ddPCR quantifying 20 molecules of BNYVV RNA1 and RNA3 was 53 and 18%, respectively. Considering these results, we define 20×10 copy number as the low limit

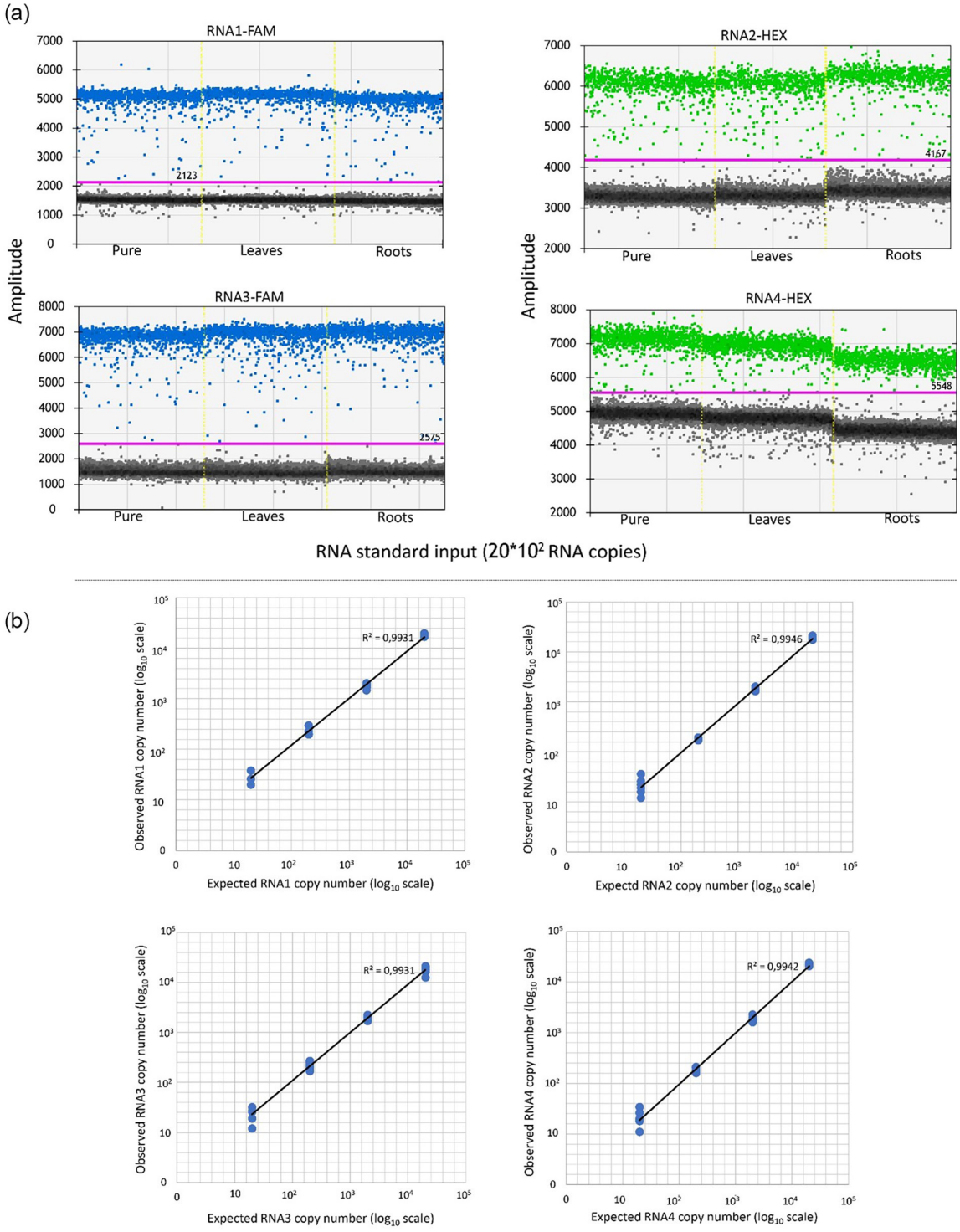

Fig. 1. Validation of two-step RT-ddPCR protocols for an absolute quantification of BNYVV RNAs. Two-step RT-ddPCR analyses were performed on four serial dilutions of BNYVV *in vitro* transcripts (20, 20x10, 20x10^2 and 20x10^3 molecules for each genomic RNA) pure or mixed with total RNAs from healthy leaf or root tissue from *C. quinoa*, *B. macrocarpa* and *S. oleracea* mixture. TaqMan probes were used to detect RNA1 and RNA3 (FAM fluorophore) and RNA2 and RNA4 (HEX fluorophore) in four separate assays. (a) Difference in fluorescence amplitude between negative and positive droplet populations from assay having as input RNA standard (pure) or mixed with leaf (leaves) or root (roots) RNA extraction: 1D dot plots show how the fluorescence signals of the positive partition populations were clearly separated from the negative populations. The pink horizontal lines represent the manually adjusted thresholds. (b) Dilution linearity of two-step RT-ddPCR results: log scatter plots having in the abscissa axis the expected BNYVV RNA copy numbers based on Qubit 3.0 and one-step RT-ddPCR quantification and, in the ordinate, the outputs of two-step RT-ddPCR. Data points represent each measurement (two replicates of each template: pure, mixed with RNA from leaves and mixed with RNA extracted from root tissue). For each BNYVV RNA, an absolute quantification scatter plot is reported as well as best fit lines and R^2 values.

Table 2. Precision and accuracy evaluations of dual-step RT-ddPCR assays are reported in the table referring to the expected copy number standard input. Precision was evaluated by calculating the relative standard deviation (RSD) in six replicates for each standard dilution whereas percentage error (PE) between expected and observed means was used to estimate the accuracy

	Precision (RSD) (%)				Accuracy (100% – PE) (%)			
Expected copy number	**RNA1**	**RNA2**	**RNA3**	**RNA4**	**RNA1**	**RNA2**	**RNA3**	**RNA4**
20×10^3	6	8	17	6	90	95	89	90
20×10^2	11	8	11	12	89	91	99	95
20×10	19	5	17	11	89	91	90	92
20	37	39	30	37	47	91	82	94

of quantification (LLQ) for our RT-ddPCR assays. Taken together, these data indicate that reverse-transcriptase events in two-step RT-ddPCR gave equimolar RNA/cDNA conversion for BNYVV RNAs above LLQ (with minimal precision and accuracy rates of 81 and 89%, respectively).

Defining BNYVV genome formula in *C. quinoa* (local host)

The quantification of BNYVV genomic RNAs in *C. quinoa*-infected plants was conducted using the two chosen BNYVV inoculum conditions described in the Methods section. These conditions included the utilization of sap extracted from infected *B. macrocarpa* leaves, as well as sap that had been enriched with RNA2 that was transcribed *in vitro*. Our previous preliminary data, which have been further substantiated in this paper, confirmed that RNA1 and RNA2 exhibit the lowest relative accumulation among the viral genomic RNAs during systemic infections in *B. macrocarpa* leaves. Consequently, an over-representation of RNA2 significantly distorts the relative frequencies of viral RNAs in the inoculum. This experimental control serves as the 'proof of concept' demonstrating that variations in the relative frequencies of its RNAs in the inoculum does not affect BNYVV genomic formula. Eight local lesions were collected and analysed for each type of inoculum. The addition of RNA2 transcripts to the inoculated sap had a statistically relevant effect on the relative accumulation of BNYVV RNA1 in total RNA extraction from *C. quinoa* lesions: the RNA1 mean relative frequency exhibited a ~108% increase when the inoculum was enriched with *in vitro*-transcribed RNA2 (Fig. 2, Table S4, available in the online version of this article). However, this kind of variation appears to be biologically negligible if we consider the conserved relative abundance pattern of BNYVV RNAs within the different *C. quinoa* loci of infection (Fig. 2): RNA3 and -4 are the two most abundant BNYVV RNA species with comparable mean relative frequencies, whereas RNA1 and -2 are at least fourfold less underrepresented. From this experiment we conclude that initial conditions of the infection may not constitute a variable determinant affecting the relative accumulation of BNYVV segments in *C. quinoa*-infected tissues. This is similar to what was shown for FBNSV genomic DNAs in *Vicia faba* [14]. *C. quinoa* SGF was determined as explained in the Methods section, calculating the mean relative frequencies of all 16-local lesion (total RNA extraction) data sets. The *C. quinoa* SGF was 2:2:12:13, where numbers indicate the stoichiometric coefficient related to the designated RNA genomic segment in the order of RNA1 : RNA2 : RNA3 : RNA4. No statistically significant differences were assessed between relative abundances of the same RNA in total and encapsidated RNA extraction (Fig. 2).

BNYVV genome formula characterization in leaves and roots of systemic hosts

To assess a possible organ effect on the SGF, BNYVV segment frequencies were determined in systemic leaves and roots of *B. macrocarpa* and *S. oleracea* host plants. No statistically significant differences were observed between BNYVV relative RNA frequencies in total and encapsidated RNA extractions in leaves of *B. macrocarpa* and *S. oleracea*, as well as in roots of *S. oleracea*, (Fig. S1). However, in *B. macrocarpa* roots, statistical differences were detected in the relative abundances of RNA1 and -4 between total and encapsidated RNA extractions. Specifically, the mean relative frequency of RNA1 in virion extraction shows a percentage increase of ~53 % compared to that calculated in total RNA extraction, while RNA4 experienced a ~17% decrease (Fig. S1 and Table S4). RNA1 and RNA2 were the two genomic species less abundant in *B. macrocarpa* and *S. oleracea* both in leaf and root tissues as previously found for *C. quinoa* infections. RNA1 and RNA2 relative frequencies in total RNA extractions ranged from ~0.08 to ~0.17 and from ~0.10 to ~0.17, respectively. RNA3 and RNA4 appeared, in general, to be more abundant in total RNA extractions but with variable mean of relative frequencies ranging from ~0.20 to ~0.36 and from ~0.38 to ~0.59 in *B. macrocarpa* and *S. oleracea*, respectively. The significant variability observed between RNA3 and RNA4 accumulation is noticeable since these RNA species cluster in heterogeneous or homogeneous groups together or with RNA1 and RNA2, depending on the organ analysed (Fig. 3a, Tables S2 and S3). In both systemic hosts, significant and substantial differences were observed for total RNA species accumulation according to the organ analysed (Figs 2a, 3b and Table S4), resulting in remarkably different segment ratios, each one specific for leaves or roots: *B. macrocarpa leaves* SGF 2:2:3:5; *B. macrocarpa roots* SGF 2:2:5:13; *S. oleracea leaves* SGF 2:2:6:6; and *S. oleracea* roots SGF 2:3:5:13.

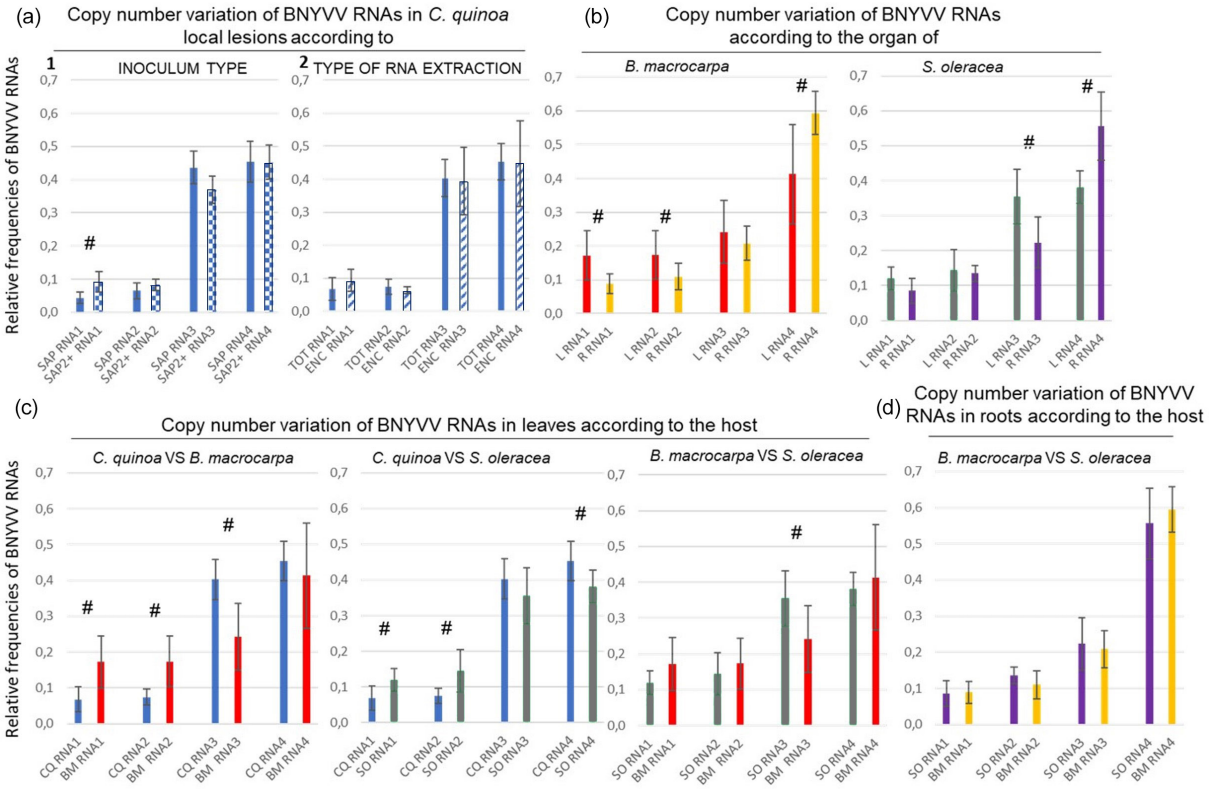

Fig. 2. Pairwise comparison of the relative frequencies of BNYVV RNAs in two groups of samples with the aim of assessing the copy number variation of each genomic RNA according to the following. (a) Inoculum type – inoculum with sap from *B. macrocarpa*-infected leaves (SAP) and inoculum with sap from *B. macrocarpa*-infected leaves with an excess of RNA2 transcribed *in vitro* (SAP2+) in local lesions of *C. quinoa* (CQ). (b) Type of RNA extraction in CQ local lesions – total RNA extraction (TOT) and encapsidated RNA extraction (ENC). (c) Organs analysed from the same host type: leaves (l) and roots (r) of *B. macrocarpa* (BM) and *S. oleracea* (SO). (d) Host type considering the same organ by making the specific comparisons: CQ-BM, CQ-SO, SO-BM for leaves (l) and SO-BM for roots (r). The histograms illustrate the average relative frequencies, with error bars indicating the standard deviation. Hash marks denote statistical differences in the relative frequencies of the same RNA within the compared sample groups. These statistical differences were calculated using Wilcoxon rank-sum tests and marked with a hash mark (#); detailed results are given in Table S4.

Differential relative genomic RNA accumulation according to BNYVV host type: *C. quinoa* vs *B. macrocarpa* vs *S. oleracea*

The influence of host type on the BNYVV SGF was verified in leaves of *C. quinoa, B. macrocarpa* and *S. oleracea* and in roots of *B. macrocarpa* and *S. oleracea*. In leaves, genome segments accumulated at significantly different frequencies in the three host species with pronounced differences involving all BNYVV RNAs (Figs 2c and 3a,Tables S2, S3 and S4). The mean relative frequencies of RNA1 and RNA2 in *C. quinoa* are ~50 % lower than in *B. macrocarpa* and *S. oleracea*, whereas RNA3 is underrepresented in *B. macrocarpa*. Interestingly, no significant variations were observed between segment relative accumulations between *B. macrocarpa* and *S. oleracea* in root tissues (Fig. 2d, Table S4).

DISCUSSION

It has been suggested that multipartite and segmented viruses adapt to different hosts or conditions by changing gene expression thanks to a gene copy number variation [14]. Such a strategy has also been associated with monopartite viruses such as *Vaccinia virus*, which responds to selection pressures experiments with the rapid amplification and duplication of K3L gene with a consequent expansion of the genome length [28]. Adaptive gene copy number variation is a common feature of prokaryotes and animal parasites, other than of viruses. Among insects, *Acyrthosiphon pisum* forms genetically distinct host-associated populations on multiple legume species thanks to copy number variation of up to 434 genes [29]. Furthermore, resistance genes are commonly amplified by many bacteria as an adaptive response to antibiotic treatment [30, 31].

To date, the unique study performed to evaluate the relative accumulation of each genomic RNA during the BNYVV infection consisted of a particle count from leaf dip preparations of *Tetragonia expansa* locally infected by isolates lacking RNA3 or RNA4 species [32]. Transmission electron microscopy (TEM) evidenced the over-representation of viral particles containing RNA3 or

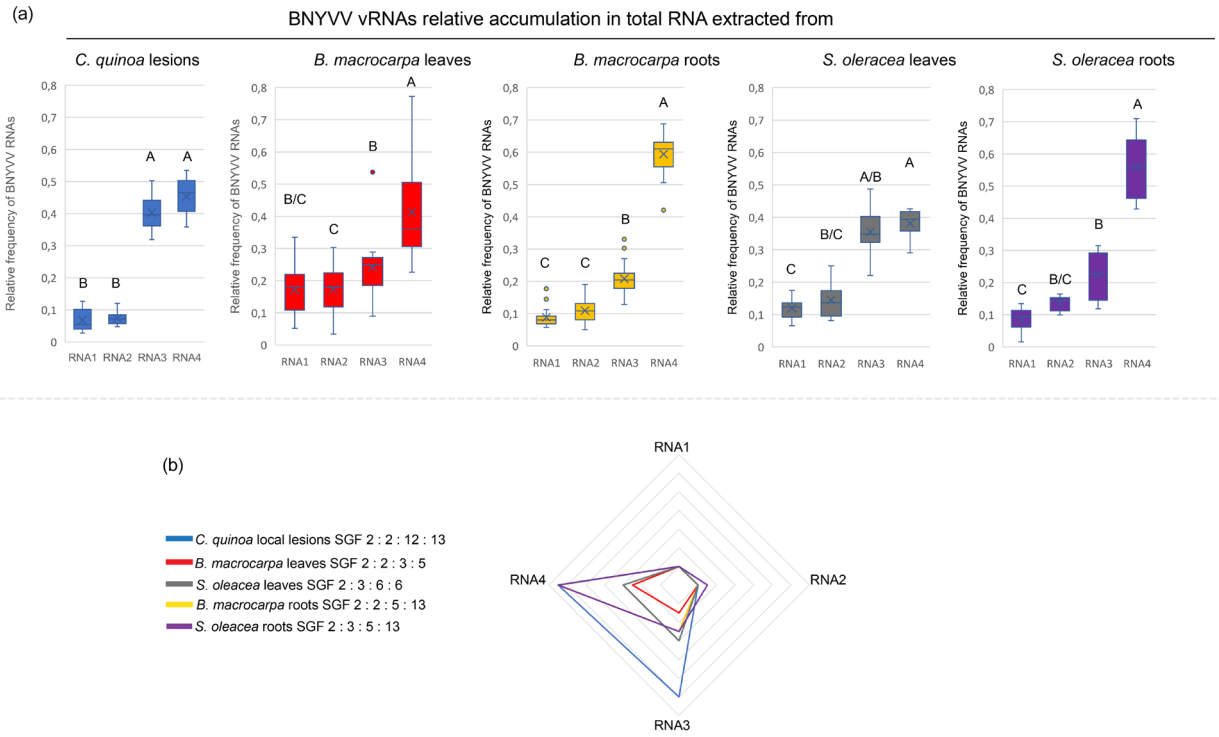

Fig. 3. BNYVV vRNAs relative accumulation in *C. quinoa* local lesions, *B. macrocarpa* and *S. oleracea* leaves and roots. (a) Descriptive boxplots of the Friedman and Wilcoxon signed-rank test analysis (Tables S2 and S3). Each boxplot represents the middle 50% of the subgroup population. The line through the box represents the median, and the cross (x) represents the mean of the sample. The lines extending from the box represent the upper and lower 25% of the data (excluding outliers). Outliers are represented by dots (°). Letters indicate significant differences between dependent variables within each group, which were estimated by Wilcoxon signed-rank test. *P*-values from the Wilcoxon signed-rank test are shown in Table S3. (b) BNYVV SGFs in *C. quinoa* (SGF *C. quinoa*) and in *B. macrocarpa* and *S. oleracea* leaves and roots (SGF *B. macrocarpa* leaves, SGF *B. macrocarpa* roots, SGF *S. oleracea* leaves and SGF *S. oleracea* roots) are noted above the radar plot comparing the different BNYVV SGFs in the different hosts and organs. Numbers indicate the stoichiometric coefficient related to the designated RNA genomic segment in the order of RNA1 : RNA2 : RNA3 : RNA4. BNYVV SGFs were calculated by pooling total RNA extraction datasets. Each RNA stoichiometric coefficient was calculated by dividing the mean of the relative frequency of the RNA by the mean of relative frequency of the less abundant RNA. SGF values were rounded to the nearest half unit.

RNA4 versus RNA1 and RNA2, the latter with similar relative amounts. Taking into account approximations due to the broken particles, *T. expansa* based on TEM findings were 2:2:12 (RNA1 : RNA2 : RNA3) and 2:4:8 (RNA1 : RNA2 : RNA4). Such local host SGF estimations from data mining support our *C. quinoa* SGF 2:2:12:13. BNYVV RNA1 and RNA2 relative frequencies remain low and comparable, with their stoichiometric ratio fixed to ~1:1 in all hosts and organs analysed. Conversely, RNA3 and RNA4 present variable stoichiometric coefficients, depending on the host and the organ. RNA3 was found to be ~6-fold more abundant than RNA1 in *C. quinoa* local lesions but just ~1.5 times more abundant in *B. macrocarpa* leaves. Similarly, RNA4 accumulated ~6.5 times more than RNA1 in *C. quinoa* local lesions and in *B. macrocarpa* and *S. oleracea* roots but only ~2.5 times more in *B. macrocarpa* leaves.

Using three different plant species, we demonstrated that while the GF appeared to be similar in *S. oleacea* and *B. macrocarpa* roots, in leaves BNYVV GF was dependent on the host. This could be explained by the soil-borne nature of the viral infection. During the BNYVV cycle, sugar beet infections are mainly restricted to the root apparatus; leaf systemic infections causing necrosis and yellowing remain rare [33, 34]. Furthermore, accessory RNA3 and -4 encode two proteins that find their *raison d'être* in the roots. RNA3-encoded P25 is responsible for the root hyper-proliferation [35], assuring in this way an increased surface for the viral acquisition and transmission by the vector *P. betae* and, therefore, transmission rate amplification. RNA4-encoded P31 plays a multifunctional role in roots, but not in leaves, by promoting vector transmission and root-specific silencing suppression [36].

Enhanced amplification of accessory RNA3 and -4 represents an interesting aspect of gene copy number influence on gene expression regulation. RNA3 expresses the pathogenic determinant p25, which is an avirulence gene triggering resistance mechanisms [37, 38]. The p25 protein expression is likely regulated during the different viral cycle steps to prevent its early expression and resulting premature cell death. This protein is efficiently expressed in the viral context of systemic host infections as well as *C. quinoa* local lesions, but it is poorly detected when translated *in vitro* from full-length RNA3 or ectopically expressed in yeast or plant using Pol-II promoter-driven expression vectors [39, 40]. As soon as viral counter defences are set, p25 expression could

start to favour the viral infection progression. Regulation of p25 expression could be dependent on a mechanism that requires a viral effector to trans-activate RNA3 translation. One could imagine a putative riboswitch motif present within the 450 nt-long 5′ UTR of the RNA3 that allows such fine-tuned regulated p25 expression. Indeed, vectors producing 5′ UTR truncated RNA3 allow efficient p25 protein production [39, 40]. Similarly, the 380 nt-long 5′ UTR present on BNYVV RNA4 may also contain such *cis* elements, allowing regulated p31 expression [39]. For these reasons, a massive replication of ancillary RNAs may not correlate to the massive translation of the encoded proteins in the early stage of infection but could be implicated in a mechanism that counteracts the plant defence system. One could argue that the increased amount of RNA3 and RNA4 could lead to a saturation of the RNA silencing machinery protecting RNA1 and RNA2 from degradation and consequently ensuring the expression of the BNYVV essential genes.

This differential accumulation of genomic RNAs also provides a theoretically high m.o.i., defined as the number of genomic segments initiating infection in a new cell. One should keep in mind, in fact, that the number of the different genome entities required for the virus to propagate in a new target cell corresponds to at least one copy of each genomic segment. On the one hand, the m.o.i. for monopartite phytoviruses ranges from 1 to 13, while on the other hand, a theoretical study assessed that four component viruses have a theoretical m.o.i. >100, assuming an equal accumulation of the genomic segments during infection [6, 41]. Accordingly, the BNYVV m.o.i. should increase to higher values to ensure the presence of RNA1 and RNA2, numerically under-represented compared to RNA3 and RNA4. Elevated m.o.i. and differential viral RNA species accumulation have direct consequences for the progression of infection and the dissemination of viral segments. Low representation of RNA1 and -2 induces biological costs probably unsustainable for the virus if the two RNAs, essential for BNYVV infection, mobilize from cell to cell in an independent manner. In support of this, dose–response curves for multipartite viruses do not follow the predictions of the independent action hypothesis model in the artificial transmission condition of leaf rub inoculation, where, for these viruses, infectivity is ensured solely by a high concentration of particles in the inoculum [42, 43]. However, in the natural context, plant viruses reach huge population sizes within their hosts but only a small proportion of genome elements found a new infection [44]. Bottlenecks occur at each level of the viral spread, from the cell-to-cell and the systemic movement to the new host transmission, and lead to genetic drift and the selection of genome variants having equal fitness [41, 45, 46].

How multipartite viruses overcome the cost of having a split genome to maintain their integrity within each infected cell during the intra and inter hosts transmission is still a matter of discussion [12, 47]. In this regard, a recent study challenges the paradigm according to which the spatial unit of the viral replication is the individual cell, demonstrating that the distinct genome element of FBNSV is mainly localized in different neighbouring cells of the sieve element companion cell complex (SECCC) [48]. FBNSV represents, however, a peculiar model of multipartite virus, since its tropism is limited to phloem tissues where the SECCC promotes the intercellular exchanges due the enhanced symplastic continuity [49]. Neighbouring phloem cells could behave like a multinucleated one, allowing genome segment replication and stabilization thanks to the facilitated trafficking of viral proteins [48]. Furthermore, aphid-mediated transmission [50] could promote the massive transmission of FBNSV virions from a donor to a recipient host. Sieve elements can act as viral reservoirs for aphid populations, favouring different rounds of infected sap feeding.

Unlike FBNSV, BNYVV demonstrates an extensive tropism moving cell to cell and over long distances, crossing cell boundaries and infecting all plant tissues [51]. Furthermore, to naturally extend the infection in new hosts the virus is transmitted by a soil-borne protozoa, whose zoospores transfer their cytoplasmic content into rootlets' infected cells [52]. Cytoplasmic sharing between infected hosts and vectors occurs at the level of a single infected cell that consequently must possess the complete set of particles. Such consideration indicates the requirement for a specific process that guarantees the coordinated movement of each segment as infective collective units. Such a process reduces the theoretical m.o.i. to the levels that are estimated in viral bottleneck size studies.

BNYVV cell-to-cell genetic drift was highlighted in *C. quinoa* for two variants of a benyvirus-derived replicon tagged with green or red fluorescent protein sequences. Mechanical leaf inoculations of the two replicons together with RNA1 and -2 produced local lesions showing either sectored expression of the marker proteins or a selection of one of the two replicons in the front of the infection [53] (and unpublished data). Assuming that replicons and RNA3 have similar amplification rates so that RNA-1 and -2 are sixfold less represented, the absence of a mixed RepIIIGFP and RepIIIRFP population within *C. quinoa*-infected cells suggests a bottleneck effect due to a specific recognition of the viral genome content within the BNYVV moving collective unit.

Funding information
M.D.A.'s work was supported by the Da Vinci programme of mobility contribution funded by the Italo-French University of Turin. The funder had no role in study design, data collection and analysis, decision to publish, or preparation of the manuscript.

Author contributions
M.D.A., D.G. and C.R. conceived the study and experiments, M.D.A., Y.G. and D.P. performed the experiments. M.D.A., D.G. and C.R. wrote the manuscript.

Conflicts of interest
The authors declare that there are no conflicts of interest.

References

1. Gabriel ML. Primitive genetic mechanisms and the origin of chromosomes. *Am Nat* 1960;94:257–269.
2. Vickerman K. Genetic systems in unicellular animals. *Sci Prog* 1966;54:13–26.
3. Jha JK, Baek JH, Venkova-Canova T, Chattoraj DK. Chromosome dynamics in multichromosome bacteria. *Biochim Biophys Acta* 2012;1819:826–829.
4. Lucía-Sanz A, Manrubia S. Multipartite viruses: adaptive trick or evolutionary treat? *NPJ Syst Biol Appl* 2017;3:34.
5. Michalakis Y, Blanc S. The curious strategy of multipartite viruses. *Annu Rev Virol* 2020;7:203–218.
6. Iranzo J, Manrubia SC. Evolutionary dynamics of genome segmentation in multipartite viruses. *Proc Biol Sci* 2012;279:3812–3819.
7. Nee S. The evolution of multicompartmental genomes in viruses. *J Mol Evol* 1987;25:277–281.
8. Chao L. Evolution of sex in RNA viruses. *J Theor Biol* 1988;133:99–112.
9. García-Arriaza J, Manrubia SC, Toja M, Domingo E, Escarmís C. Evolutionary transition toward defective RNAs that are infectious by complementation. *J Virol* 2004;78:11678–11685.
10. Ojosnegros S, García-Arriaza J, Escarmís C, Manrubia SC, Perales C, *et al*. Viral genome segmentation can result from a trade-off between genetic content and particle stability. *PLoS Genet* 2011;7:e1001344.
11. McDonald SM, Nelson MI, Turner PE, Patton JT. Reassortment in segmented RNA viruses: mechanisms and outcomes. *Nat Rev Microbiol* 2016;14:448–460.
12. Sicard A, Michalakis Y, Gutiérrez S, Blanc S. The strange lifestyle of multipartite viruses. *PLoS Pathog* 2016;12:e1005819.
13. Hu Z, Zhang X, Liu W, Zhou Q, Zhang Q, *et al*. Genome segments accumulate with different frequencies in *Bombyx mori bidensovirus*. *J Basic Microbiol* 2016;56:1338–1343.
14. Sicard A, Yvon M, Timchenko T, Gronenborn B, Michalakis Y, *et al*. Gene copy number is differentially regulated in a multipartite virus. *Nat Commun* 2013;4:2248.
15. Gallet R, Fabre F, Michalakis Y, Blanc S. The number of target molecules of the amplification step limits accuracy and sensitivity in ultradeep-sequencing viral population studies. *J Virol* 2017;91:e00561-17.
16. Wu B, Zwart MP, Sánchez-Navarro JA, Elena SF. Within-host evolution of segments ratio for the tripartite genome of Alfalfa mosaic virus. *Sci Rep* 2017;7:5004.
17. Yu N-T, Xie H-M, Zhang Y-L, Wang J-H, Xiong Z, *et al*. Independent modulation of individual genomic component transcription and a cis-acting element related to high transcriptional activity in a multipartite DNA virus. *BMC Genomics* 2019;20:573.
18. Zhao W, Wang Q, Xu Z, Liu R, Cui F. Distinct replication and gene expression strategies of the *Rice Stripe virus* in vector insects and host plants. *J Gen Virol* 2019;100:877–888.
19. Boezen D, Johnson ML, Grum-Grzhimaylo AA, van der Vlugt RA, Zwart MP. Evaluation of sequencing and PCR-based methods for the quantification of the viral genome formula. *Virus Res* 2023;326:199064.
20. Adams MJ, Adkins S, Bragard C, Gilmer D, Li D, *et al*. ICTV virus taxonomy profile: *Virgaviridae*. *J Gen Virol* 2017;98:1999–2000.
21. Tamada T, Kondo H, Chiba S. Genetic diversity of beet necrotic yellow vein virus. In: *Rhizomania*. Cham: Springer International Publishing, . pp. 109–131.
22. Delbianco A, Lanzoni C, Klein E, Rubies Autonell C, Gilmer D, *et al*. Agroinoculation of *Beet necrotic yellow vein virus* cDNA clones results in plant systemic infection and efficient *Polymyxa betae* transmission. *Mol Plant Pathol* 2013;14:422–428.
23. Quillet L, Guilley H, Jonard G, Richards K. *In vitro* synthesis of biologically active beet necrotic yellow vein virus RNA. *Virology* 1989;172:293–301.
24. Ziegler-Graff V, Bouzoubaa S, Jupin I, Guilley H, Jonard G, *et al*. Biologically active transcripts of Beet necrotic yellow vein virus RNA-3 and RNA-4. *Journal of General Virology* 1988;69:2347–2357.
25. Jupin I, Richards K, Jonard G, Guilley H, Pleij CW. Mapping sequences required for productive replication of beet necrotic yellow vein virus RNA 3. *Virology* 1990;178:273–280.
26. Nolan T, Hands RE, Bustin SA. Quantification of mRNA using real-time RT-PCR. *Nat Protoc* 2006;1:1559–1582.
27. Ståhlberg A, Håkansson J, Xian X, Semb H, Kubista M. Properties of the reverse transcription reaction in mRNA quantification. *Clin Chem* 2004;50:509–515.
28. Elde NC, Child SJ, Eickbush MT, Kitzman JO, Rogers KS, *et al*. Poxviruses deploy genomic accordions to adapt rapidly against host antiviral defenses. *Cell* 2012;150:831–841.
29. Duvaux L, Geissmann Q, Gharbi K, Zhou J-J, Ferrari J, *et al*. Dynamics of copy number variation in host races of the pea aphid. *Mol Biol Evol* 2015;32:63–80.
30. San Millan A, Santos-Lopez A, Ortega-Huedo R, Bernabe-Balas C, Kennedy SP, *et al*. Small-plasmid-mediated antibiotic resistance is enhanced by increases in plasmid copy number and bacterial fitness. *Antimicrob Agents Chemother* 2015;59:3335–3341.
31. Sandegren L, Andersson DI. Bacterial gene amplification: implications for the evolution of antibiotic resistance. *Nat Rev Microbiol* 2009;7:578–588.
32. Tamada T, Shirako Y, Abe H, Saito M, Kiguchi T, *et al*. Production and pathogenicity of isolates of beet necrotic yellow vein virus with different numbers of RNA components. *J Gen Virol* 1989;70:3399–3409.
33. Tamada T, Baba T. Beet necrotic yellow vein virus from Rizomania-affected sugar beet in Japan. *Jpn J Phytopathol* 1973;39:325–332.
34. McGrann GRD, Grimmer MK, Mutasa-Göttgens ES, Stevens M. Progress towards the understanding and control of sugar beet rhizomania disease. *Mol Plant Pathol* 2009;10:129–141.
35. Peltier C, Schmidlin L, Klein E, Taconnat L, Prinsen E, *et al*. Expression of the *beet necrotic yellow vein virus* p25 protein induces hormonal changes and a root branching phenotype in *Arabidopsis thaliana*. *Transgenic Res* 2011;20:443–466.
36. Rahim MD, Andika IB, Han C, Kondo H, Tamada T. RNA4-encoded p31 of beet necrotic yellow vein virus is involved in efficient vector transmission, symptom severity and silencing suppression in roots. *J Gen Virol* 2007;88:1611–1619.
37. Chiba S, Miyanishi M, Andika IB, Kondo H, Tamada T. Identification of amino acids of the beet necrotic yellow vein virus p25 protein required for induction of the resistance response in leaves of *Beta vulgaris* plants. *J Gen Virol* 2008;89:1314–1323.
38. Thiel H, Varrelmann M. Identification of Beet necrotic yellow vein virus P25 pathogenicity factor-interacting sugar beet proteins that represent putative virus targets or components of plant resistance. *Mol Plant Microbe Interact* 2009;22:999–1010.
39. Gilmer D. Molecular biology and replication of beet necrotic yellow vein virus. In: *Rhizomania*. Cham: Springer International Publishing, . pp. 85–107.
40. Peltier C, Klein E, Hleibieh K, D'Alonzo M, Hammann P, *et al*. Beet necrotic yellow vein virus subgenomic RNA3 is a cleavage product leading to stable non-coding RNA required for long-distance movement. *J Gen Virol* 2012;93:1093–1102.
41. Gallet R, Fabre F, Thébaud G, Sofonea MT, Sicard A, *et al*. Small bottleneck size in a highly multipartite virus during a complete infection cycle. *J Virol* 2018;92:e00139-18.
42. Fulton RW. The effect of dilution on necrotic ringspot virus infectivity and the enhancement of infectivity by noninfective virus. *Virology* 1962;18:477–485.
43. Price WC, Spencer EL. Accuracy of the local lesion method for measuring virus activity. II. Tobacco-necrosis, alfalfa-mosaic, and tobacco-ringspot viruses. *Am J of Bot* 1943;30:340–346.

44. Gutiérrez S, Zwart MP. Population bottlenecks in multicomponent viruses: first forays into the uncharted territory of genome-formula drift. *Curr Opin Virol* 2018;33:184–190.
45. Ali A, Roossinck MJ. Genetic bottlenecks during systemic movement of *Cucumber mosaic virus* vary in different host plants. *Virology* 2010;404:279–283.
46. Miyashita S, Kishino H. Estimation of the size of genetic bottlenecks in cell-to-cell movement of *soil-borne wheat mosaic virus* and the possible role of the bottlenecks in speeding up selection of variations in *trans*-acting genes or elements. *J Virol* 2010;84:1828–1837.
47. Dall'Ara M, Ratti C, Bouzoubaa SE, Gilmer D. Ins and outs of multipartite positive-strand RNA plant viruses: packaging versus systemic spread. *Viruses* 2016;8:228.
48. Sicard A, Pirolles E, Gallet R, Vernerey M-S, Yvon M, *et al*. A multicellular way of life for a multipartite virus. *Elife* 2019;8:e43599.
49. Van Bel AJE. The phloem, a miracle of ingenuity. *Plant Cell Environ* 2003;26:125–149.
50. Sicard A, Zeddam J-L, Yvon M, Michalakis Y, Gutiérrez S, *et al*. Circulative nonpropagative aphid transmission of nanoviruses: an oversimplified view. *J Virol* 2015;89:9719–9726.
51. Tamada T, Kondo H, Bouzoubaa S. Pattern of systemic movement of soil-borne plant viruses: evidence obtained from GFP-tagged Beet necrotic yellow vein virus. In: *Proc Ninth Symp Int Work Group Plant Viruses Fungal Vectors Obihiro Hokkaido Jpn 19–22 August 2013*. 2013. pp. 11–14.
52. Peltier C, Hleibieh K, Thiel H, Klein E, Bragard C, *et al*. Molecular biology of the Beet necrotic yellow vein virus. *Plant Viruses* 2008;2:14–24.
53. Ratti C, Hleibieh K, Bianchi L, Schirmer A, Autonell CR, *et al*. *Beet soil-borne mosaic virus* RNA-3 is replicated and encapsidated in the presence of BNYVV RNA-1 and -2 and allows long distance movement in *Beta macrocarpa*. *Virology* 2009;385:392–399.